ACS ES&T Water

pubs.acs.org/estwater

Article

Disproportionate Changes in Composition and Molecular Size Spectra of Dissolved Organic Matter between Influent and Effluent from a Major Metropolitan Wastewater Treatment Plant

Hui Lin, Kazuaki Matsui, Ryan J. Newton, and Laodong Guo*

Cite This: ACS EST Water 2022, 2, 216−225

Read Online

ACCESS | Metrics & More | Article Recommendations | Supporting Information

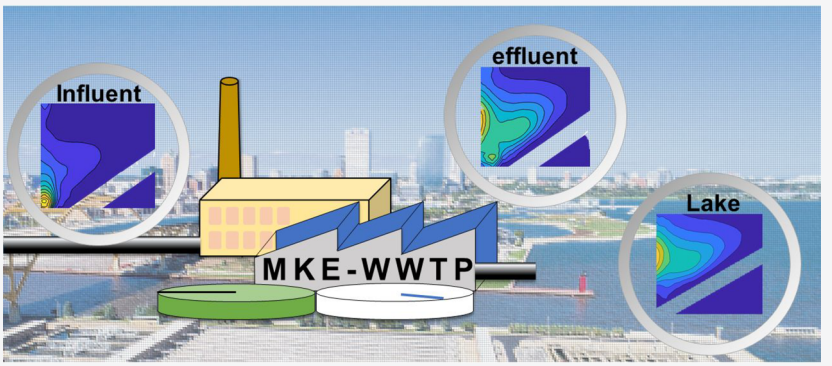

ABSTRACT: Dynamic changes in the abundance, composition, and size spectra of dissolved organic matter (DOM) in different size-fractions between influent and effluent from Milwaukee metropolitan wastewater treatment plants (WWTPs) were evaluated using size-fractionation, excitation−emission matrix (EEM) coupled with parallel factor analysis (PARAFAC), and ΔEEM approaches. Up to 82.7% of DOC, 43.1% of total dissolved nitrogen (TDN), and 52.4% of chromophoric-DOM (CDOM) were removed from the influent, indicating different reactivity/degradability and disproportionate removal between DOM species. Within the CDOM pool, both the aromaticity and humification-index increased after treatments while the biological-index remained similar, showing a preferential removal of autochthonous DOM and the protein-like components, resulting in a higher abundance of humic-like components in the effluent but little change in the DOM size spectra. Up to 3%−5% differences were measured in the bulk DOM concentrations between the 0.22 and 0.7 μm filtrates. In addition, DOM in the 0.22−0.7 μm size-fraction contained almost only protein-like components, showing a high DOM heterogeneity. High levels of photochemically and biologically labile DOM in the effluent, with a higher molecular weight and lower DOC/TDN ratio, may alter the microbial community and biogeochemical processes in coastal Lake Michigan. Long-term and concurrent characterization of DOM in both effluent and receiving waters is needed to better understand the environmental/ecological roles of DOM as it moves through WWTPs and into the natural environment.

KEYWORDS: *dissolved organic matter, fluorescence EEM-PARAFAC, molecular weight distribution, size-dependent DOM properties, WWTP effluent*

INTRODUCTION

Dissolved organic matter (DOM) is ubiquitous in aquatic environments and is a heterogeneous mixture of organic compounds and components with diverse molecular sizes, compositions, and reactivities.[1−3] Compared with freshwater ecosystems, such as rivers and lakes,[4,5] DOM is more concentrated in the influent of wastewater treatment plants (WWTPs) with a unique chemical composition.[6,7] Both pretreatment sewage and WWTP effluent are released regularly to the environment, and concurrent characterization of DOM in both the influent and effluent of WWTPs and receiving waters is needed to better understand the potential impacts of wastewater and effluent on aquatic environments. Indeed, DOM from the effluent of major metropolitan WWTPs can significantly influence the water quality, microbial community composition, and biogeochemical processes in the receiving aquatic ecosystems.[8,9] In addition, DOM in water treatment has the potential to form or to be transformed to disinfection byproducts.[10,11] Thus, the abundance, composition, and

Received: October 12, 2021
Revised: November 13, 2021
Accepted: November 22, 2021
Published: December 2, 2021

chemical properties of DOM are valuable indicators for wastewater treatment performance and the impacts of effluent on water quality and environmental health in receiving aquatic environments.[6,7,12] The majority of DOM in the influent is expected to be removed during treatments in WWTPs, but specific changes in DOM quantity and quality, including composition and size spectra, between the influent and effluent have scarcely been characterized concurrently.

Fluorescence spectroscopy techniques have been widely used to characterize DOM in natural waters and sewer waters. Excitation−emission matrix (EEM) coupled with parallel factor analysis (PARAFAC) has proven to be a useful tool to elucidate DOM properties in wastewater.[6,13] The size or molecular weight distribution of DOM is another important demension in the characterization of DOM. In aquatic environments, the fluorescent composition and optical properties of DOM are closely related to its molecular weights, with humic-like DOM mostly partitioned in lower molecular weight or nanocolloidal size-fractions and protein-like DOM and carbohydrate components mostly in higher molecular weight fractions.[2,3] Similarly, molecular weight distributions of DOM have been characterized in the influent and effluent of WWTPs using size exclusion chromatography.[13−15] Nevertheless, studies detailing changes in DOM size spectra and fluorescent composition during wastewater treatments remain few. Little is known about the detailed characteristics of DOM in the size-fraction between 0.22 and 0.7 μm in the influent and effluent. The specific fluorescence characteristics of the removed DOM components in the course of sewage treatment have not been shown explicitly.

In this study, DOM samples from influent and effluent of WWTPs in Milwaukee Metropolitan Sewerage District were characterized for different DOM species, including dissolved organic carbon (DOC), total dissolved nitrogen (TDN), chromophoric DOM (CDOM), and fluorescence DOM (FDOM), as well as DOM size distributions using asymmetrical flow field-flow fractionation (FlFFF). In addition, ΔEEM was employed to elucidate the fluorescence characteristics in the removed/degraded DOM fractions and in the 0.22−0.7 μm DOM size-fraction on the basis of differences in the EEMs between the influent and effluent and between the 0.7 and 0.22 μm filtrates, respectively. We also compare DOM composition and chemical properties between the effluent and receiving waters, including the Milwaukee estuary and Lake Michigan.

Our objectives were to evaluate (1) the representativeness of bulk DOM using different filtrates (i.e., the <0.22 vs <0.7 μm) and the removal efficiency of bulk DOC and specific DOM components during wastewater treatment, (2) dynamic changes in DOM composition, optical properties, and molecular size spectra before and after wastewater treatment and thus the biological reactivity or degradability of different DOM components, and (3) potential impacts of effluent on the receiving water environment on the basis of comparisons in their DOM quantity and quality. Results from this study provide an improved understanding of the relative lability and resistance of different DOM components and molecular size-fractions during wastewater treatments. Furthermore, we provide perspectives on what DOM components are available to photolysis and to the organisms living in the aquatic ecosystems recieiving municipal wastewater effluent.

MATERIALS AND METHODS

Sample Collection. Flow-proportional 24 h composite water samples were collected in autoclaved 500 mL polypropylene bottles from inlets and outlets of Jones Island Water Reclamation Facility (JI) and South Shore Water Reclamation Facility (SS) in Milwaukee, Wisconsin. Both JI and SS WWTPs also discharge effluent directly into Lake Michigan, a primary drinking water source for over 12 million people lake-wide. Although the two treatment plants service the same city, JI is a combined sewer system while SS is a separated sewer system, so this provides further insight into the DOM characteristics of combined vs separated systems.

Weekly samples were collected between December 18th, 2019 and February 18th, 2020 from both WWTPs. A total of 56 samples including the influent and effluent were collected. Samples were filtered through either 0.7 μm GF/F glass microfiber filters (Whatman) or 0.22 μm mixed cellulose ester membrane filters (Millipore). Both the <0.7 and <0.22 μm filtrates were collected from selected samples for DOM characterization to evaluate differences in quantity, chemical properties, and molecular size spectra of DOM between the two filtrates.

Measurements of DOC, TDN, and UV-Absorbance. Concentrations of DOC (in mg-C/L) and TDN (in mg-N/L) were measured on a Shimadzu TOC-L analyzer coupled with a total nitrogen detector (TNM-L). Samples were acidified to pH ≤ 2 with concentrated HCl after sample collection. The detection limit was 0.01 mg-C/L, and precision in terms of coefficient of variation was ≤2%.[16] Ultrapure water and certified DOC samples (from the University of Miami) were run as samples to monitor the performance of the instrument.[17]

UV−visible absorption spectra were obtained using an Agilent 8453 spectrophotometer with a 10 mm quartz cuvette over the wavelength range from 220 to 900 nm. Ultrapure water was used as a blank, and the refractive index effect was corrected.[18,19] The absorption coefficient at a specific wavelength λ (a_λ) was calculated as $a_\lambda = 2.303 \times A_\lambda/l$, where A_λ is the absorbance at λ (nm) and l (m) is the light path length of the cuvette. The a_{254} was commonly recognized as the measure of CDOM.[18] Spectral slope ($S_{275-295}$) was calculated using a linear regression method to fit absorbance spectra ranging from 275 to 295 nm:

$$a_\lambda = a_{280} e^{-S_{275-295}(\lambda-280)}$$

where λ is the wavelength, a_{280} is the absorption coefficient at 280 nm, and $S_{275-295}$ is the spectral slope between 275 and 295 nm, which is inversely correlated with DOM molecular weight within a specific ecosystem.[20] Specific UV absorbance at 254 nm ($SUVA_{254}$, in L mg^{-1} m^{-1}), an indicator of aromaticity,[18] was calculated as $SUVA_{254} = A_{254}/DOC$, where A_{254} is the absorbance at 254 nm.

Fluorescence EEM-PARAFAC Analysis. Fluorescence EEM spectra were obtained using a spectrofluorometer (Horiba Fluoromax-4) in 3D scan mode with a 10 mm quartz cuvette. Samples were scanned at excitation wavelengths (λ_{Ex}) ranging from 220 to 480 nm with a 5 nm increment and emission wavelengths (λ_{Em}) ranging from 260 to 600 nm with a 2 nm increment. First-order and second-order of the Rayleigh scattering peaks and Raman scattering peaks were removed before PARAFAC analysis.[21] A series of quinine sulfate solutions were used to calibrate the instrument, and

https://doi.org/10.1021/acsestwater.1c00391
ACS EST Water 2022, 2, 216−225

Table 1. Comparisons in DOC (mg-C L^{-1}), TDN (mg-N L^{-1}), a_{254} (m^{-1}), and $SUVA_{254}$ (L mg-C^{-1} m^{-1}), Biological Index (BIX), and Humification Index (HIX) between the 0.22 and 0.7 μm Filtrates and between the Influent and Effluent of MMSD's Jones Island (JI) and South Shore (SS) facilities, as well as Δ-Values of Each Parameter between Influent and Effluent, with Positive Δ Values (+) Denoting an Increase in the Effluent while Negative Δ Values Indicating a Decrease in That Parameter in the Effluent after Treatments[a]

	Example I				Example II			
sampling site	JI		SS		JI		SS	
	<0.7 μm	<0.22 μm	<0.7 μm	<0.22 μm	<0.7 μm	<0.22 μm	<0.7 μm	<0.22 μm
				DOC (mg-C L^{-1})				
influent	72.07	66.55	50.52	41.70	49.09	47.70	63.52	61.30
effluent	9.45	8.10	12.15	7.22	8.08	8.04	12.16	11.99
Δ(DOC)	−62.62	−58.45	−38.37	−34.48	−41.01	−39.66	−51.36	−49.31
removal (%)	86.9	87.8	75.9	82.7	83.5	83.1	80.9	80.6
				TDN (mg-N L^{-1})				
influent	19.65	18.05	21.47	20.87	13.47	12.78	24.61	24.00
effluent	7.08	7.19	13.86	13.59	8.61	8.68	14.12	14.16
Δ(TDN)	−12.57	−10.86	−7.61	−6.98	−4.86	−4.10	−10.49	−9.84
removal (%)	63.9	60.2	35.4	33.4	36.1	32.1	42.6	41.0
				a_{254}(m^{-1})				
influent	55.41	53.64	55.41	52.68	55.32	53.04	73.02	64.98
effluent	29.64	28.87	29.64	24.60	25.90	24.87	34.80	34.17
Δ(a_{254})	−25.77	−24.77	−28.50	−28.08	−29.42	−28.17	−38.22	−30.81
removal (%)	46.5	46.2	52.9	53.3	69.6	53.1	52.3	47.4
				$SUVA_{254}$(L mg-$C^{1-}m^{-1}$)				
influent	0.77	0.76	1.06	1.07	1.74	1.11	1.19	1.02
effluent	3.13	3.56	2.19	2.09	3.22	3.07	2.90	2.81
Δ(SUVA)	+2.36	+2.80	+1.13	+1.02	+1.48	+1.96	+1.71	+1.79
				BIX				
influent	0.96	0.97	0.86	0.94	0.83	0.83	0.99	1.03
effluent	0.87	0.88	0.87	0.91	0.85	0.90	0.92	0.94
Δ(BIX)	−0.11	−0.10	+0.02	−0.04	+0.05	+0.07	−0.08	−0.08
				HIX				
influent	0.36	0.37	0.53	0.53	0.38	0.39	0.46	0.47
effluent	0.70	0.67	0.77	0.74	0.73	0.71	0.70	0.69
Δ(HIX)	+0.34	+0.30	+0.24	+0.24	+0.34	+0.31	+0.24	+0.22

[a]Examples shown here are those from both JI and SS facilities collected on January 29, 2020 (Example I) and February 19, 2020 (Example II).

quinine sulfate equivalent (QSE) was used as the unit of fluorescence intensities.[5] Biological index (BIX) and humification index (HIX) are indicators of autochthonous and allochthonous DOM sources, respectively, and were calculated from fluorescence intensities at different λ_{Em} values.[22]

Both PARAFAC analysis using the drEEM toolbox (version 0.5.0)[21] and statistical tests were performed in the Matlab (R2020b) platform to mathematically deconvolute the EEM database, a total of 90 EEM spectra (56 influent/effluent plus 34 size-fractionated samples), into different fluorescent DOM components. Half-split validation was used to validate the EEM-PARAFAC models.[3,23]

Size Distribution of DOM Analyzed Using Flow Field-Flow Fractionation. DOM size distributions were characterized using an asymmetrical FlFFF system (AF2000, Postnova) coupled with a UV-absorbance detector (SPD-20A, Shimadzu) and two fluorescence detectors (RF-20A, Shimadzu). The poly(ether sulfone) membrane in the separation channel has a manufacturer-rated pore-size of 0.3 kDa. The carrier solution was made of 10 mM NaCl and 5 mM H_3BO_3 and adjusted to pH 8 with NaOH, which has been proven as the optimal carrier for natural water samples.[24] Flow settings used for the FlFFF analysis are given in Table S1. Before sample measurements, the retention time of DOM in the FlFFF system was calibrated under the same instrument conditions using standard macromolecular organic compounds (proteins) with a known molecular weight (Table S2). The relationship between FlFFF retention time and diffusion coefficient was established on the basis of the calibration with protein standards, and thus, hydrodynamic diameter (in nm) or molecular weight (in kDa) can be converted from a diffusion coefficient on the basis of Stokes law.[24,25] A UV-absorbance detector measured the absorbance at 254 nm, while the two fluorescence detectors targeted $\lambda_{Ex}/\lambda_{Em}$ at 350/450 and 275/340 nm, representing humic-like and protein-like fluorophores, respectively. A series of qunine solfate solutions (in parts per billion) were used to calibrate the fluorescence detectors, and the fluorescence intensities are expressed in quinine sulfate equivalent (ppb-QSE).[24] Other detailed analytical procedures and data acquisition are described elsewhere.[3,24]

Statistical Analyses. Statistical analyses were performed using the Matlab statistics toolbox (MathWorks, R2020a), with a p-value <0.01 as statistically significant.

RESULTS AND DISCUSSION

Differences in Bulk DOM Properties between Influent and Effluent. The concentrations of DOC and TDN as well

https://doi.org/10.1021/acsestwater.1c00391
ACS EST Water 2022, 2, 216−225

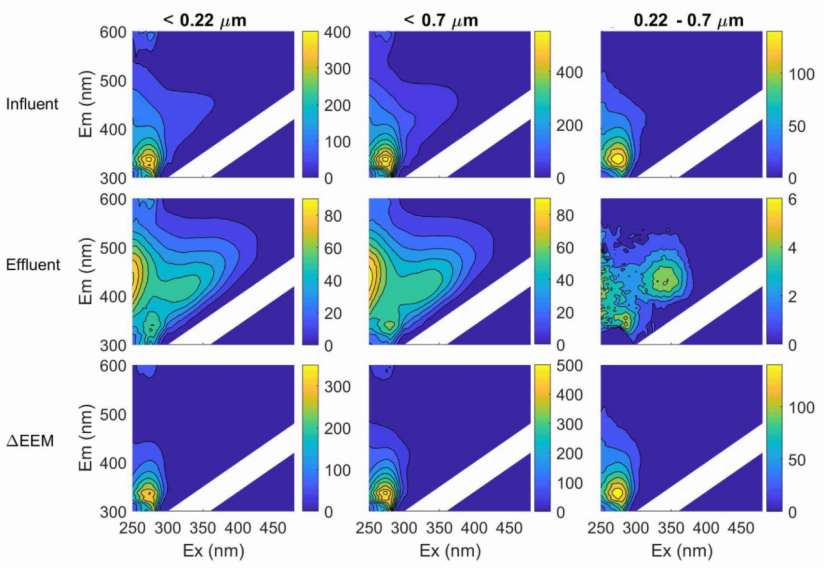

Figure 1. Examples of fluorescence excitation emission matrix (EEM) spectra of different DOM size-fractions, including <0.22, < 0.7, and 0.22−0.7 μm, in the influent (top panels) and effluent (middle panels) as well as the EEM spectra of DOM that were removed from the <0.22, < 0.7, and 0.22−0.7 μm size-fractions in the influent during treatments (bottom panels) derived from ΔEEM on the basis of the difference in EEM data between the influent and effluent.

as optical properties including a_{254} and $SUVA_{254}$ are listed in Table 1 for comparisons between the 0.22 and 0.7 μm filtrates and between influent and effluent samples collected from the JI and SS. As shown in Table 1, concentrations of DOC and TDN in the influent samples varied considerably depending on the filter pore-size used, sampling date, and sampling sites or wastewater treatment plants. Similarly, both a_{254} and $SUVA_{254}$ values in the influent samples also varied markedly between filtrates and sampling dates, showing distinct differences in influent's DOM quantity and quality with time (Table 1). Most importantly, vast differences, both positive and negative, in all parameters were observed between the influent and effluent. On average, up to 82.7 ± 3.6% of the bulk DOC and 43 ± 12% of TDN had been removed after treatment on the basis of the concentration differences between influent and effluent samples (Table 1). For CDOM, about 49.8 ± 3.4% of CDOM (a_{254}) was removed in the course of treatments, which suggested that a larger portion (up to 50%) of the bulk CDOM pool is microbially refractory during wastewater treatment compared to only <20% recalcitrant in the DOC pool. The disproportionate removal rates between bulk DOC and CDOM pools indicate that bulk DOM in wastewaters is highly heterogeneous in lability and reactivity. As a result, values of $SUVA_{254}$, an indicator of DOM aromaticity, increased after treatment, implying that the less biodegradable DOM components are mostly the highly aromatic DOM components. This result is consistent with those observed in degradation experiments using natural DOM samples.[2,26] The removal rate of TDN was highly variable, ranging from 32% to 64%, likely depending on the relative abundance of dissolved organic nitrogen (DON) and dissolved inorganic nitrogen (DIN) as well as denitrification/nitrification processes during the watsewater treatments.[27]

In addition to bulk DOM concentrations, other intensive optical properties (independent to concentrations) also demonstrated a consistent change, either positive or negative between the influent and effluent samples (Table 1). While values of BIX had a small and variable change between the influent and effluent, both HIX and $SUVA_{254}$ values increased significantly (t test: $p < 0.01$) after wastewater treatment, indicating again that aromatic DOM components are less microbially degradable.

Changes in EEM Spectra of DOM between Influent and Effluent. Examples of fluorescence EEM spectra are shown in Figure 1 for influent and effluent samples in the 0.22 and 0.7 μm filtrates and the 0.22−0.7 μm DOM size-fraction. The difference in EEM spectra between influent and effluent or the EEM spectra of the removed-DOM is also presented for comparisons (Figure 1). Characteristic fluorescence peaks in these EEM spectra include peaks A, C, T, and B (Table S3). As expected, the major DOM components characterized in the EEM spectra are distinct between the influent and effluent samples regardless of filtrates in the <0.22, < 0.7, or the 0.22−0.7 μm fractions (Figure 1). Specifically, the major EEM peak in the influent is peak T with its Ex/Em centered at 275/340 nm.[28] In contrast, after treatments, the predominant DOM component becomes humic-like or peak A with a maximum Ex/Em at 250/430 nm. Changes in both fluorescence intensities and major DOM components between the influent and effluent samples indicate that, on average, 65.5% of the fluorescent signatures are removed after treatment, and the major DOM component shifts from mostly protein-like in the influent to largely humic-like in the effluent. The shift in major DOM components between influent and effluent attests to the fact that humic-like DOM components can persist and thus accumulate during microbial degradation, while protein-like components are preferentially decomposed during wastewater treatment, giving rise to an increase in the relative abundance of humic-like DOM (Figure 1). This conclusion also is supported by the observed changes in HIX and $SUVA_{254}$ between the influent and effluent samples (Table 1).

The ΔEEM spectra derived from the differences in EEM spectra between the influent and effluent samples clearly and consistently show that the DOM components being removed during wastewater treatment are largely the protein-like DOM components with Ex/Em maximum at 275/340 nm regardless

https://doi.org/10.1021/acsestwater.1c00391
ACS EST Water 2022, 2, 216−225

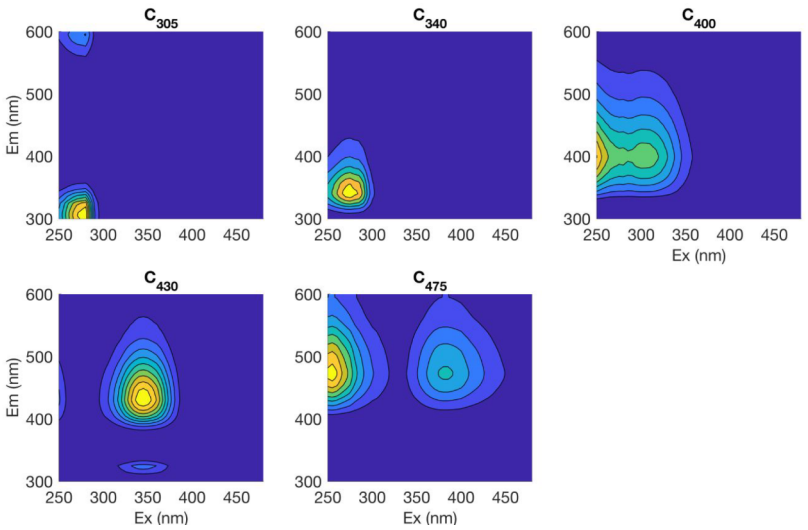

Figure 2. EEM contours of the PARAFAC-derived fluorescent DOM components on the basis of 90 samples, including 56 influent/effluent and 34 size-fractionated samples, from both Jones Island and South Shore WWTP facilities.

Table 2. Comparisons in the Relative Abundance, Δ-Values, and Removal % of Fluorescent DOM Components As Well As the Protein-Like to Humic-Like Components Ratio between the <0.22 μm and <0.7 μm Filtrates and between the Influent and Effluent of MMSD's Jones Island (JI) and South Shore (SS) Facilities[a]

	Example I				Example II			
sampling site	JI		SS		JI		SS	
filtrate size cutoff (μm)	<0.7	<0.22	<0.7	<0.22	<0.7	<0.22	<0.7	<0.22
				C_{305}				
inf	504.1	415.0	292.2	254.3	406.2	274.5	512.5	437.8
eff	51.5	39.2	13.2	5.9	33.2	25.1	53.5	40.7
ΔC_{305}	−452.6	−375.8	−279.0	−248.5	−373.0	−249.4	−459.0	−397.1
removal (%)	89.8	90.6	95.5	97.7	91.8	90.9	89.6	90.7
				C_{340}				
inf	338.1	328.6	245.0	257.3	314.9	257.1	332.8	314.2
eff	51.8	77.8	43.9	69.7	36.5	51.8	98.7	122.0
ΔC_{340}	−286.3	−250.7	−201.1	−187.6	−278.4	−205.3	−234.1	−192.2
removal (%)	84.7	76.3	82.1	72.9	88.4	79.8	70.3	61.2
				C_{400}				
inf	156.5	141.9	194.6	187.4	133.7	103.2	221.9	207.6
eff	80.3	73.6	82.1	80.5	71.7	69.6	114.5	109.9
ΔC_{400}	−76.3	−68.3	−112.4	−106.8	−62.0	−33.6	−107.4	−97.7
removal (%)	48.7	48.1	57.8	57.0	46.4	32.6	48.4	47.1
				C_{430}				
inf	65.9	53.2	104.6	63.4	47.5	37.8	85.7	61.1
eff	49.7	39.7	47.2	39.1	38.2	33.5	62.9	54.2
ΔC_{430}	−16.2	−13.5	−57.5	−24.4	−9.3	−4.2	−22.8	−6.9
removal (%)	24.6	25.4	54.9	38.4	19.6	11.2	26.6	11.2
				C_{475}				
inf	67.1	62.4	90.2	86.2	69.1	57.5	105.1	96.5
eff	58.7	55.1	50.2	49.5	46.8	46.1	79.9	77.9
ΔC_{475}	−8.4	−7.3	−40.0	−36.7	−22.3	−11.4	−25.2	−18.5
removal (%)	12.5	11.7	44.4	42.6	32.3	19.8	24.0	19.2
				$(C_{305} + C_{340})/(C_{400} + C_{430} + C_{475})$				
inf	2.9	2.9	1.4	1.5	2.9	2.7	2.0	2.1
eff	0.5	0.7	0.3	0.4	0.4	0.5	0.6	0.7
δratio	−2.4	−2.2	−1.1	−1.1	−2.4	−2.2	−1.5	−1.4

[a]Δ-values are the differences of each component or parameter between the influent and effluent, with positive Δ-values (+) denoting an increase in the effluent while negative Δ-values indicate a decrease in the parameter in the effluent after treatments. Examples shown here are based on samples took from both JI and SS facilities on January 29, 2020 (Example I) and February 19, 2020 (Example II).

https://doi.org/10.1021/acsestwater.1c00391
ACS EST Water 2022, 2, 216−225

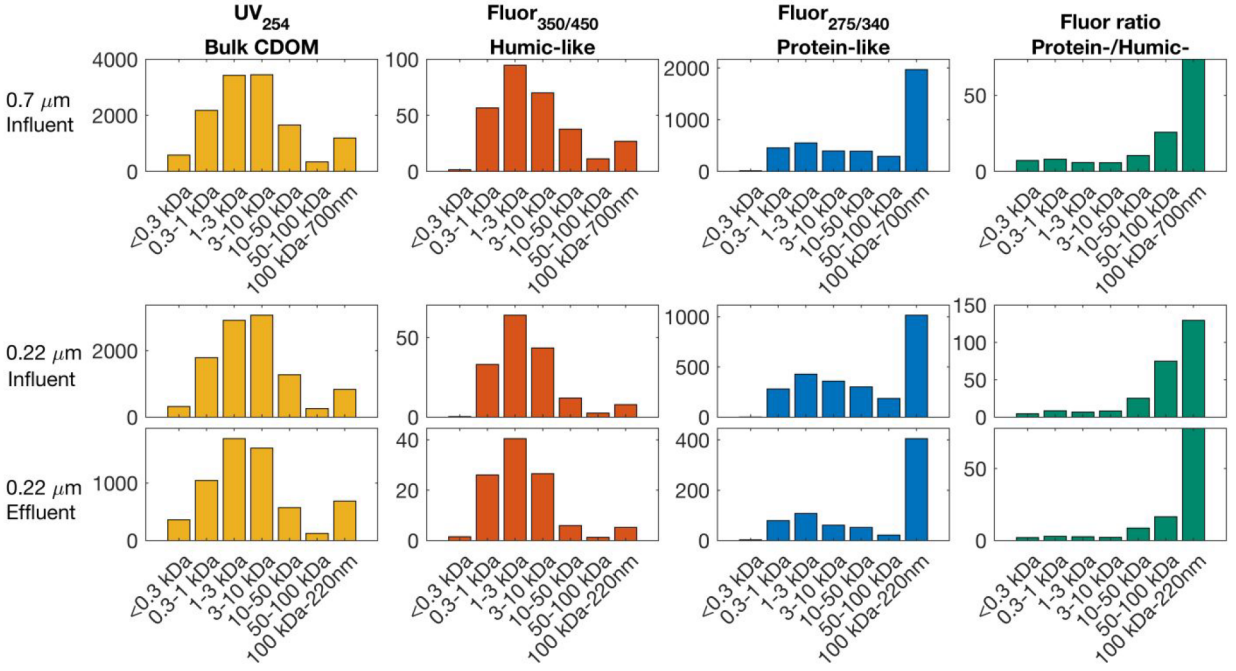

Figure 3. Examples showing the molecular weight distributions of the bulk CDOM (or UV_{254}), humic-like components (Ex/Em = 350/450 nm), and protein-like components (Ex/Em = 275/340 nm) in the 0.22 μm and 0.7 μm filtrates between the influent and effluent and variations in the protein-like/humic-like ratio with DOM molecular weight (based on samples collected on 19-Feb-2020).

of DOM size fractions (Figure 1, bottom panels). The DOM composition-dependent degradation pathways observed here are consistent with recent studies on DOM in natural waters.[2,26,29]

Characterization of DOM in Municipal Wastewaters. PARAFAC analysis was used to decompose the EEM spectra into five major fluorescent DOM components, including components C_{305}, C_{340}, C_{400}, C_{430}, and C_{475} (Figure 2) with their specific Ex/Em maxima listed in Table S4. Examples showing the relative abundance of each PARAFAC-derived DOM component are given in Table 2. Components were named after their characteristic emission wavelengths; for instance, C_{305} has an emission peak at 305 nm, which covers the Peak B, a protein-like fluorescent component.[28] C_{340} is a protein-like fluorescent component as well, which has characteristics of Peak T.[28] These two protein-like DOM components are associated with 34.9% and 33.7% of the total fluorescence intensities, respectively. The other three PARAFAC-derived components are all humic-like fluorescent components that have been widely observed in freshwater ecosystems.[30] Overall, C_{400} contributes 15.9% of total fluorescence intensities, while C_{430} and C_{475} have the least contributions to the total fluorescence signatures (comprising 6.74% and 8.77%, respectively) in all samples.

In the influent samples, the protein-like DOM components are predominated with 37.1% C_{305} and 34.6% C_{340}, while the three humic-like DOM components cumulatively comprise only 28.3% of the total fluorescence intensities. Compared with the influent samples, protein-like C_{305} and C_{340} components in the effluent samples decreased considerabaly to 10.2% and 24.1%, while C_{400}, C_{430}, and C_{475} increased to 29.5%, 15.6%, and 20.6%, respectively (Figure S1). The PARAFAC-derived fluorescent components and their relative abundances in wastewaters identified here are distinctively different from those reported for freshwater environments adjacent to the treatment plants, such as the Milwaukee River,[31] coastal Lake Michigan,[5] and other U.S. rivers.[4,19] However, after treatment, the EEM characteristics of DOM in the effluent become more similar to those of natural waters, with the major difference being the remaining protein-like components in the effluent.

As shown in Table 2, up to 92.5% and 80.3% of the protein-like components, C_{305} and C_{340}, in the influent were eliminated during treatments. These results are similar to those previously reported.[32] The humic-like DOM components also show a significant removal of their initial signatures (48.3%, 26.5%, and 25.8% for C_{400}, C_{430}, and C_{475}, respectively), but to a lesser extent then the protein-like components (Table 2). On the basis of changes in component ratios, values of $(C_{305} + C_{340})/(C_{400} + C_{430} + C_{475})$, the ratio of total protein-like to humic-like components, decreased significantly between influent and effluent regardless of sampling sites, filtrates, or sampling dates (Table 2), from an average of 2.3 ± 0.6 in the influent to 0.5 ± 0.1 in effluent. This again supports the conclusion that protein-like DOM components are indeed preferentially removed during wastewater treatment.

Changes in DOM Size Spectra between Influent and Effluent. In addition to changes in the concentration and composition of DOM during treatments (Figure 1 for EEM), concurrent changes in the molecular size distribution of DOM could be expected although less quantified. Examples of FlFFF fractograms are given in Figure S2 to show continuous size spectra of different DOM components, including UV absorbance representing bulk CDOM as well as fluorescent humic-like and protein-like components in influent and effluent samples. Both bulk CDOM and humic-like components simply had a major peak centered at ~3 kDa regardless of effluent or influent. Protein-like components, on the contrary, contained not only a major peak in nanocolloidal size region with a shoulder extending to 10 kDa but also a secondary peak at the >100 kDa size range (Figure S2).

https://doi.org/10.1021/acsestwater.1c00391
ACS EST Water 2022, 2, 216−225

Compared to the influent samples, the protein-like DOM ($Fluor_{275/340}$) in effluent samples had much lower fluorescence intensities in both the major peak in the nanocolloidal size range and the secondary peak for large colloids, but without the shoulder peak for median molecular size-fractions in effluent samples. In other words, fluorescence intensities in both middle-size and larger-size protein-like components were significantly reduced after treatments. In contrast, the size spectra (or peak shape) of both bulk CDOM and humic-like components changed little between the influent and effluent after treatments even though their UV-absorbance and fluorescence intensities decreased by 34% and 27%, respectively (Figure S2). Little change in the size spectra of humic-like DOM components is likely due to their unique molecular size characteristics, mainly in the nanocolloidal size range,[33] and their lower biodegradability (Figure 1).

Similarly, the molecular weight distributions of different DOM components, using histogram diagrams integrated from continuous FlFFF fractograms, show a major peak around the 1−10 kDa size range and a secondary peak in the 100 kDa-220 nm (or 700 nm) size-fraction (Figure 3). In general, the molecular weight distributions are somewhat similar between bulk CDOM (UV_{254}) and fluorescent humic-like components ($Fluor_{350/450}$) in both influent and effluent samples. There existed a quasi-normal distribution in the molecular size spectra with a peak at the 1−10 kDa for the bulk CDOM and 1−3 kDa for the fluorescent humic-like components (Figure 3 and Figure S2). For the protein-like components, in addition to a peak centered at the 1−3 kDa size fraction, their predominant peak is at the >100 kDa, showing a bimodal size distribution in the DOM size spectra. This bimodal size distribution observed for the protein-like components here is consistent with those observed for other natural water samples,[3,33,34] indicating that the protein-like DOM contains not only amino acids associated chromophores but also high-molecular-weight (HMW) sticky protein-like components. On the contrary, both bulk CDOM and humic-like components had a single peak size-distribution and partitioned mostly in the lower molecular weight or nanocolloidal fractions, consistent with the nature of humic substances, such as the highly dispersive detergent-type properties and highly dispersive.[35]

When the ratio of the protein-like to the humic-like fluorescence intensities (P/H) at each DOM size-interval was plotted against DOM molecular weight ranges, a general increase in the P/H ratio with DOM molecular weight was observed (Figure 3). The P/H ratio in the 1−10 kDa size range is as low as <5 but as high as 129 in the >100 kDa size-fraction. This result attests to a highly heterogeneous nature of DOM in wastewater, similar to those observed for DOM in the aquatic continuum.[1,3] Furthermore, changes in the size spectra of DOM components during treatments can be quantified on the basis of the difference in FlFFF fractograms between the influent and effluent (Figure S3). For both bulk CDOM (UV_{254}) and humic-like components, the removed-DOM components are exclusively the nanosized DOM fractions <20 kDa. On the contrary, the protein-like components being removed are the size-fractions containing not only the nanosize and midsize DOM ranging from 0.5 to 20 kDa but also the large-size DOM > 100 kDa. Overall, the DOM components removed during wastewater treatment had their molecular weight with peak intensity at the ≤1 kDa for the bulk CDOM and at the 1−3 kDa for humic-like DOM, while the removed protein-like DOM not only had a major peak with a molecular weight of ∼1 kDa but also contained minor components with molecular sizes >100 and even >1000 kDa (Figure S3).

Differences in Composition and Size Spectra between the <0.22 and <0.7 μm Filtrates. Both the 0.22 and 0.7 μm filters have been commonly adopted in studies of DOM in natural and engineered systems.[36−38] In addition, the composition and reactivity of DOM and their environmental fate and cycling pathways have been shown to be highly related to DOM molecular sizes.[1−3] Nevertheless, the difference in DOM quantity and quality between the 0.22 μm filtrate and the 0.7 μm filtrate remains poorly quantified.[39] On the basis of the difference in pore sizes, the 0.7 μm filtrate should theoretically contain more DOM or have a higher DOC concentration than the 0.22 μm filtrate. Unsurprisingly, concentrations or values of DOC, TDN, and CDOM (a_{254}) in the 0.7 μm filtrate are all consistently higher than those in the 0.22 μm filtrate (Table 1, t tests: $p < 0.01$). On average, DOC, TDN, and CDOM in the 0.7 μm filtrate were 5.0%, 3.2%, and 4.8% higher than those in the 0.2 μm filtrate, respectively, although DOM concentrations in the 0.7 μm are likely underestimated due to the potential adsorption of DOM onto GF/F filters.[36,40] Similar differences in the quantity of bulk DOM resulting from membrane pore-size differences have been reported for natural waters.[39,41] Therefore, consistently using the same pore size and type of filters is important in the characterization of bulk DOM, allowing for data comparisons between time-series samples and between studies despite DOM being highly operationally defined and dependent on the filter pore size used in the filtration.

Other optical properties, such as $SUVA_{254}$, BIX, and HIX, on the contrary, show little or less differences between the 0.22 and 0.7 μm filtrates (t tests: $p > 0.1$, Table 1), indicating that the additional 3%−5% bulk DOM between the 0.22 and 0.7 μm may not significantly alter the intensitive chemical properties of the bulk DOM pool due to their overall high DOM concentrations. It seems that the difference in filter pore sizes can result in a significant difference in DOM concentrations or extensive properties whose values are proportional to the quantity of DOM in the filtrate but less so in intensive properties whose values are not related to DOM quantity, such as $SUVA_{254}$, BIX, and HIX. However, differences in DOM composition and size spectra and thus DOM lability and reactivity occur between the 0.22 and 0.7 μm filtrates.

Although EEM contours of the 0.22 and 0.7 μm filtrates are highly similar (Figure 1), their major fluorescent DOM components are evidently different from those of the 0.22−0.7 μm DOM size-fraction, especially in the effluent. As depicted in the ΔEEM (Figure 1 right panels), the fluorescent DOM composition of the 0.22−0.7 μm size-fraction is also related to the sources of water. For example, the 0.22−0.7 μm filtrate in the influent samples contains mostly protein-like DOM components. The same filtrate in the effluent samples, in contrast, contains mostly humic-like DOM (peak C) in addition to protein-like components (peak T).

Regarding differences in size spectra, DOM in the <0.7 μm filtrate not only had higher fluorescence intensities but also contained more HMW-DOM components in the FlFFF fractograms compared to the <0.22 μm filtrate (Figure 3). For example, both the humic-like and protein-like DOM components exhibited a visibly higher shoulder peak in the <0.7 μm filtrate sample. In addition, protein-like DOM

https://doi.org/10.1021/acsestwater.1c00391
ACS EST Water 2022, 2, 216−225

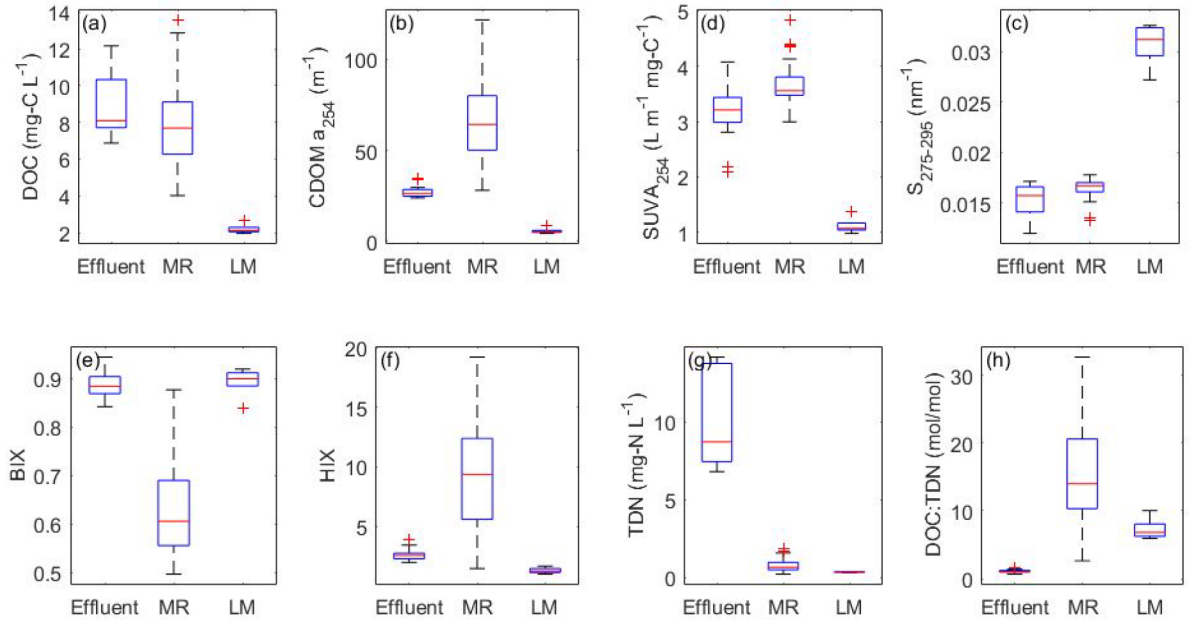

Figure 4. Comparisons in DOM properties between the effluent (n = 57), lower Milwaukee River water (MR, n = 48), and Lake Michigan water (LM, n = 5) for (a) DOC, (b) CDOM a_{254}, (c) SUVA$_{254}$, (d) $S_{275-295}$, (e) BIX, (f) HIX, (g) TDN, and (h) DOC/TDN ratio. The box and bar are interquartile (25% and 75%) and median, respectively. Whisker depict the most extreme data point that is no more than 1.5-fold the interquartile range. Outliers are shown with cross symbols (+).

components in the <0.7 μm filtrate also had a larger portion of DOM in the >50 nm size-fraction. Clearly, this is consistent with the fact that the <0.7 μm filtrate contains not only DOM < 0.22 μm but also microbes or measurable large sized-DOM fractions between 0.22 and 0.7 μm. Therefore, bulk DOM containing a continuous molecular size spectrum is highly dependent on the filter pore size used in isolating dissolved from the particulate phase.[39]

Comparisons in DOM Properties between Effluent and Receiving Waters. The impacts of effluent DOM on receiving water are a public concern depending on the composition and reactivity of DOM in the effluent. The effluent from the WWTP at Jones Island is discharged into the Milwaukee Harbor−Lake Michigan region, where the Milwaukee River, Kinnickkinnic River, and Menomonee River mix with coastal Lake Michigan waters. Concentrations of DOC in the JI effluent are slightly lower than those of the lower Milwaukee River[31] but are significantly higher than those in Lake Michigan (Figure 4). Similarly, a_{254} values in the effluent are significantly lower than those in the Milwaukee River but higher than those in Lake Michigan (Figure 4).[5] The same variation trend is observed for SUVA$_{254}$ values (Figure 4), with a similar aromaticity level between the effluent and river water but much higher than that of Lake Michigan. Spectral slope ($S_{275-295}$) values followed the order of effluent < Milwaukee River < Lake Michigan (Figure 4), showing a change in DOM molecular weight or biological/chemical reacivity in the order of effluent > Milwaukee River > Lake Michigan on the basis of the DOM size-reactivity continuum model.[1] Comparisons in fluorescence indices show a similar biological index (BIX) between the effluent and Lake Michigan waters, which are much higher than those of Milwaukee River waters, again suggesting that DOM from the effluent is of higher biological reactivity than river waters. In addition, a higher humification index (HIX) and higher aromaticity (SUVA$_{254}$) in the effluent than those in Lake Michigan waters point to a higher photochemical reactivity once discharged into Lake Michigan. TDN in the effluent is considerably higher than the receiving waters, while the DOC/TDN ratios in the effluent are lower than those in both Lake Michigan and the Milwaukee River (Figure 4), consistently indicating biologically labile DOM in the effluent.

Overall, compared to the receiving waters, the effluent contained an elevated DOC, a much higher TDN, and a variable CDOM. In addition, in light of chemical composition and reactivity, DOM from the effluent is of higher molecular weight, lower DOC/TDN ratio, and higher BIX and thus higher biological lability compared to Milwaukee River and Lake Michigan waters. The overall impacts of WWTP-effluent on the receiving environment may be related to the fluxes of effluent, but the biologically labile DOM with a higher molecular weight and lower DOC/TDN ratio could have a potential disproportionate influence on microbial community, algal blooms, and biogeochemical processes in coastal southern Lake Michigan.

CONCLUSIONS

In this study, we found that, in the course of sewerage treatments, DOM was removed dispropornately depending on the chemical properties and reactivity/lability of specific DOM components. Although >80% of the bulk DOC could be removed from the influent by WWTPs, only about half of CDOM in the influent was removed. Within the CDOM pool, the biologically or microbially labile protein-like DOM was preferentially removed compared to other fluorescent components, resulting in an accumulation of humic-like DOM in the effulent. Molecular size distributions or size spectra of DOM had little change between the influent and effluent, likely due to their overall high DOM abundances compared to most natural waters. However, the size spectra were distinct between different DOM components (e.g., humic-like vs protein-like). A detectable difference in DOM

https://doi.org/10.1021/acsestwater.1c00391
ACS EST Water 2022, 2, 216−225

abundance and fluorescent components between the <0.22 and <0.7 μm filtrates was observed for the first time showing that almost only protein-like components appear in the 0.22−0.7 μm size-fraction, pointing to a highly heterogeneous nature between DOM size-fractions and the need to characterize the size-dependent composition of DOM and their environmental behavior and fate. The discharge of WWTP's effluent with DOM containing a low DOC/TDN ratio, more higher molecular weight, and more photochemically and biologically labile components could have a significant impact on receiving waters, influencing microbial community and biogeochemical cycling, especially in coastal Lake Michigan, an oligotrophic ecosystem. Further studies are needed to quantitatively evaluate the potential impacts from effluent.

■ ASSOCIATED CONTENT

Supporting Information

The Supporting Information is available free of charge at https://pubs.acs.org/doi/10.1021/acsestwater.1c00391.

Figures of changes in the relative abundances of each DOM component, FlFFF fractograms, and size distribution and tables of instrument settings for FlFFF analysis, protein standards used for the calibration of our FlFFF system, fluorescence intentities of major peaks in EEM spectra, and characteristics of the PARAFAC-derived major fluorescent DOM components and their specific Ex/Em wavelengths (PDF)

■ AUTHOR INFORMATION

Corresponding Author

Laodong Guo − *School of Freshwater Sciences, University of Wisconsin-Milwaukee, Milwaukee, Wisconsin 53204, United States*; Phone: 414-382-1742; Email: guol@uwm.edu

Authors

Hui Lin − *School of Freshwater Sciences, University of Wisconsin-Milwaukee, Milwaukee, Wisconsin 53204, United States*

Kazuaki Matsui − *School of Freshwater Sciences, University of Wisconsin-Milwaukee, Milwaukee, Wisconsin 53204, United States; Department of Civil and Environmental Engineering, Kindai University, Osaka 577-8502, Japan*

Ryan J. Newton − *School of Freshwater Sciences, University of Wisconsin-Milwaukee, Milwaukee, Wisconsin 53204, United States*; orcid.org/0000-0001-8946-0035

Complete contact information is available at: https://pubs.acs.org/10.1021/acsestwater.1c00391

Notes

The authors declare no competing financial interest.

■ ACKNOWLEDGMENTS

The authors gratefully thank Deb Dila, Melinda Bootsma, and staff members at the MMSD's reclamation facilities for their assistance in sample collection, the editor and two anomynous reviwers for their constructive comments, which improved the manuscript, and support from the University of Wisconsin−Milwaukee (DIG-101 × 405), Freshwater Collaborative of Wisconsin (Track 2), Milwaukee County Parks, China Scholarship Council (#201606310069 to H.L.), and the UWM's Distinguished Dissertator Fellowship (to H.L.).

■ REFERENCES

(1) Benner, R.; Amon, R. M. W. The Size-Reactivity Continuum of Major Bioelements in the Ocean. *Annual Review of Marine Science* **2015**, *7* (1), 185−205.

(2) Xu, H.; Guo, L. Intriguing Changes in Molecular Size and Composition of Dissolved Organic Matter Induced by Microbial Degradation and Self-Assembly. *Water Res.* **2018**, *135*, 187−194.

(3) Lin, H.; Guo, L. Variations in Colloidal DOM Composition with Molecular Weight within Individual Water Samples as Characterized by Flow Field-Flow Fractionation and EEM-PARAFAC Analysis. *Environ. Sci. Technol.* **2020**, *54* (3), 1657−1667.

(4) Spencer, R. G. M.; Butler, K. D.; Aiken, G. R. Dissolved Organic Carbon and Chromophoric Dissolved Organic Matter Properties of Rivers in the USA. *J. Geophys. Res.* **2012**, *117* (G3), 1−14.

(5) Zhou, Z.; Guo, L.; Minor, E. C. Characterization of Bulk and Chromophoric Dissolved Organic Matter in the Laurentian Great Lakes during Summer 2013. *J. Great Lakes Res.* **2016**, *42* (4), 789−801.

(6) Yang, L.; Han, D. H.; Lee, B. M.; Hur, J. Characterizing Treated Wastewaters of Different Industries Using Clustered Fluorescence EEM-PARAFAC and FT-IR Spectroscopy: Implications for Downstream Impact and Source Identification. *Chemosphere* **2015**, *127*, 222−228.

(7) Choi, P. M.; O'Brien, J. W.; Tscharke, B. J.; Mueller, J. F.; Thomas, K. V.; Samanipour, S. Population Socioeconomics Predicted Using Wastewater. *Environ. Sci. Technol. Lett.* **2020**, *7*, 567.

(8) Costa, A.; Schaider, L.; Hughes, P. *Pollution in the Coastal Zone: A Case Study of Wastewater on Cape Cod, MA*; Elsevier Inc., 2018.

(9) Su, Z.; Li, A.; Chen, J.; Huang, B.; Mu, Q.; Chen, L.; Wen, D. Wastewater Discharge Drives ARGs Spread in the Coastal Area: A Case Study in Hangzhou Bay, China. *Mar. Pollut. Bull.* **2020**, *151*, 110856.

(10) Bridgeman, J.; Bieroza, M.; Baker, A. The Application of Fluorescence Spectroscopy to Organic Matter Characterisation in Drinking Water Treatment. *Rev. Environ. Sci. Bio/Technol.* **2011**, *10* (3), 277−290.

(11) Li, L.; Wang, Y.; Zhang, W.; Yu, S.; Wang, X.; Gao, N. New Advances in Fluorescence Excitation-Emission Matrix Spectroscopy for the Characterization of Dissolved Organic Matter in Drinking Water Treatment: A Review. *Chem. Eng. J.* **2020**, *381*, 122676.

(12) Kikuchi, T.; Fujii, M.; Terao, K.; Jiwei, R.; Lee, Y. P.; Yoshimura, C. Correlations between Aromaticity of Dissolved Organic Matter and Trace Metal Concentrations in Natural and Effluent Waters: A Case Study in the Sagami River Basin, Japan. *Sci. Total Environ.* **2017**, *576*, 36−45.

(13) Komatsu, K.; Onodera, T.; Kohzu, A.; Syutsubo, K.; Imai, A. Characterization of Dissolved Organic Matter in Wastewater during Aerobic, Anaerobic, and Anoxic Treatment Processes by Molecular Size and Fluorescence Analyses. *Water Res.* **2020**, *171*, 115459.

(14) Imai, A.; Fukushima, T.; Matsushige, K.; Kim, Y.; Choi, K. Characterization of Dissolved Organic Matter in Effluents from Wastewater Treatment Plants. *Water Res.* **2002**, *36* (4), 859−870.

(15) Ignatev, A.; Tuhkanen, T. Monitoring WWTP Performance Using Size-Exclusion Chromatography with Simultaneous UV and Fluorescence Detection to Track Recalcitrant Wastewater Fractions. *Chemosphere* **2019**, *214*, 587−597.

(16) Guo, L.; Santschi, P. H.; Warnken, K. Dynamics of Dissolved Organic Carbon (DOC) in Oceanic Environments. *Limnol. Oceanogr.* **1995**, *40* (8), 1392−1403.

(17) Zhou, Z.; Guo, L. Evolution of the Optical Properties of Seawater Influenced by the Deepwater Horizon Oil Spill in the Gulf of Mexico. *Environ. Res. Lett.* **2012**, *7* (2), 025301.

(18) Weishaar, J. L.; Aiken, G. R.; Bergamaschi, B. A.; Fram, M. S.; Fujii, R.; Mopper, K. Evaluation of Specific Ultraviolet Absorbance as an Indicator of the Chemical Composition and Reactivity of Dissolved Organic Carbon. *Environ. Sci. Technol.* **2003**, *37* (20), 4702−4708.

(19) DeVilbiss, S. E.; Zhou, Z.; Klump, J. V.; Guo, L. Spatiotemporal Variations in the Abundance and Composition of Bulk and

Chromophoric Dissolved Organic Matter in Seasonally Hypoxia-Influenced Green Bay, Lake Michigan, USA. *Sci. Total Environ.* **2016**, *565*, 742−757.
(20) Fichot, C. G.; Benner, R. A Novel Method to Estimate DOC Concentrations from CDOM Absorption Coefficients in Coastal Waters. *Geophys. Res. Lett.* **2011**, *38* (3), 1.
(21) Murphy, K. R.; Stedmon, C. A.; Graeber, D.; Bro, R. Fluorescence Spectroscopy and Multi-Way Techniques. PARAFAC. *Anal. Methods* **2013**, *5* (23), 6557.
(22) Huguet, A.; Vacher, L.; Relexans, S.; Saubusse, S.; Froidefond, J. M.; Parlanti, E. Properties of Fluorescent Dissolved Organic Matter in the Gironde Estuary. *Org. Geochem.* **2009**, *40* (6), 706−719.
(23) Stedmon, C. A.; Bro, R. Characterizing Dissolved Organic Matter Fluorescence with Parallel Factor Analysis: A Tutorial. *Limnol. Oceanogr.: Methods* **2008**, *6*, 572−579.
(24) Zhou, Z.; Guo, L. A Critical Evaluation of an Asymmetrical Flow Field-Flow Fractionation System for Colloidal Size Characterization of Natural Organic Matter. *Journal of Chromatography A* **2015**, *1399*, 53−64.
(25) Stolpe, B.; Guo, L.; Shiller, A. M.; Hassellöv, M. Size and Composition of Colloidal Organic Matter and Trace Elements in the Mississippi River, Pearl River and the Northern Gulf of Mexico, as Characterized by Flow Field-Flow Fractionation. *Mar. Chem.* **2010**, *118* (3−4), 119−128.
(26) Chen, M.; Jaffé, R. Quantitative Assessment of Photo- and Bio-Reactivity of Chromophoric and Fluorescent Dissolved Organic Matter from Biomass and Soil Leachates and from Surface Waters in a Subtropical Wetland. *Biogeochemistry* **2016**, *129* (3), 273−289.
(27) Chai, H.; Xiang, Y.; Chen, R.; Shao, Z.; Gu, L.; Li, L.; He, Q. Enhanced Simultaneous Nitrification and Denitrification in Treating Low Carbon-to-Nitrogen Ratio Wastewater: Treatment Performance and Nitrogen Removal Pathway. *Bioresour. Technol.* **2019**, *280*, 51−58.
(28) Coble, P. G. Marine Optical Biogeochemistry: The Chemistry of Ocean Color. *Chem. Rev.* **2007**, *107*, 402−418.
(29) Carstea, E. M.; Bridgeman, J.; Baker, A.; Reynolds, D. M. Fluorescence Spectroscopy for Wastewater Monitoring: A Review. *Water Res.* **2016**, *95*, 205−219.
(30) Murphy, K. R.; Timko, S. A.; Gonsior, M.; Powers, L. C.; Wünsch, U. J.; Stedmon, C. A. Photochemistry Illuminates Ubiquitous Organic Matter Fluorescence Spectra. *Environ. Sci. Technol.* **2018**, *52* (19), 11243−11250.
(31) Lin, H. Molecular Weight Distributions and Size-dependent Composition of Dissolved Organic Matter in the Aquatic Continuum. Ph.D. Dissertation, University of Wisconsin-Milwaukee, Milwaukee, WI, 2021.
(32) Yang, L.; Hur, J.; Zhuang, W. Occurrence and Behaviors of Fluorescence EEM-PARAFAC Components in Drinking Water and Wastewater Treatment Systems and Their Applications: A Review. *Environ. Sci. Pollut. Res.* **2015**, *22* (9), 6500−6510.
(33) Stolpe, B.; Guo, L.; Shiller, A. M. Binding and Transport of Rare Earth Elements by Organic and Iron-Rich Nanocolloids in Alaskan Rivers, as Revealed by Field-Flow Fractionation and ICP-MS. *Geochim. Cosmochim. Acta* **2013**, *106*, 446−462.
(34) Zhou, Z.; Stolpe, B.; Guo, L.; Shiller, A. M. Colloidal Size Spectra, Composition and Estuarine Mixing Behavior of DOM in River and Estuarine Waters of the Northern Gulf of Mexico. *Geochim. Cosmochim. Acta* **2016**, *181*, 1−17.
(35) von Wandruszka, R. Humic Acids: Their Detergent Qualities and Potential Uses in Pollution Remediation. *Geochem. Trans.* **2000**, *1* (2), 10.
(36) Morán, X. A. G.; Gasol, J. M.; Arin, L.; Estrada, M. A Comparison between Glass Fiber and Membrane Filters for the Estimation of Phytoplankton POC and DOC Production. *Mar. Ecol.: Prog. Ser.* **1999**, *187*, 31−41.
(37) Knefelkamp, B.; Carstens, K.; Wiltshire, K. H. Comparison of Different Filter Types on Chlorophyll-a Retention and Nutrient Measurements. *J. Exp. Mar. Biol. Ecol.* **2007**, *345* (1), 61−70.
(38) Turner, C. R.; Barnes, M. A.; Xu, C. C. Y.; Jones, S. E.; Jerde, C. L.; Lodge, D. M. Particle Size Distribution and Optimal Capture of Aqueous Macrobial EDNA. *Methods in Ecology and Evolution* **2014**, *5* (7), 676−684.
(39) Xu, H.; Guo, L. Molecular Size-Dependent Abundance and Composition of Dissolved Organic Matter in River, Lake and Sea Waters. *Water Res.* **2017**, *117*, 115−126.
(40) Maske, H.; Garcia-Mendoza, E. Adsorption of Dissolved Organic Matter to the Inorganic Filter Substrate and Its Implications for 14C Uptake Measurements. *Appl. Environ. Microbiol.* **1994**, *60* (10), 3887−3889.
(41) Nimptsch, J.; Woelfl, S.; Kronvang, B.; Giesecke, R.; González, H. E.; Caputo, L.; Gelbrecht, J.; von Tuempling, W.; Graeber, D. Does Filter Type and Pore Size Influence Spectroscopic Analysis of Freshwater Chromophoric DOM Composition? *Limnologica* **2014**, *48*, 57−64.

https://doi.org/10.1021/acsestwater.1c00391
ACS EST Water 2022, 2, 216−225